

# Fibrous Dysplasia of Bone in the McCune-Albright Syndrome

## Abnormalities in Bone Formation

Mara Riminucci,\* Larry W. Fisher,\*  
Andrew Shenker,<sup>†</sup> Allen M. Spiegel,<sup>†</sup>  
Paolo Bianco,<sup>‡</sup> and Pamela Gehron Robey\*

From the Craniofacial and Skeletal Diseases Branch,\* National Institute of Dental Research, and the Metabolic Diseases Branch,<sup>‡</sup> National Institute of Diabetes, Digestive and Kidney Diseases, National Institutes of Health Bethesda, Maryland, and the Division of Pathology,<sup>†</sup> Department of Experimental Medicine, University of L'Aquila and Department of Experimental Medicine, University of Rome "La Sapienza", Rome, Italy

**In addition to café-au-lait pigmentation patterns and hyperendocrinopathies, fibrous dysplasia of bone is a major finding in the McCune-Albright syndrome. Activating missense mutations of the *Gsα* gene leading to overactivity of adenyl cyclase have been identified in patients with McCune-Albright syndrome, but the mechanism leading to the specific development of fibrous dysplasia in bone has not been elucidated. By means of specific peptide antisera and reverse transcriptase polymerase chain reaction *in situ* hybridization, we show that expression of *Gsα* and its mRNA is critically up-regulated during maturation of precursor osteogenic cells to normal osteoblast cells and that this pattern of expression is retained in fibrous dysplasia. A functional characterization of fibrous dysplastic tissues revealed that the fibrotic areas consist, in fact, of an excess of cells with phenotypic features of pre-osteogenic cells, whereas the lesional bone formed *de novo* within fibrotic areas represents the biosynthetic output of mature but abnormal osteoblasts. These cells are noted for peculiar changes in cell shape and interaction with matrix, which were mimicked *in vitro* by the effects of excess exogenous cAMP on human osteogenic cells. Osteoblasts involved with the *de novo* deposition of lesional bone in fibrous dysplasia produce a bone matrix enriched in certain anti-adhesion molecules (versican and osteonectin), and poor in the pro-adhesive molecules osteopontin and bone sialoprotein, which is in contrast to the high levels of these two proteins found in normal *de novo* bone. Our data indicate the need to reinterpret fibrous dysplasia of bone as a disease of cells in the osteogenic lineage,**

**related to the effects of excess cAMP on bone cell function. They further suggest that a critical, physiological, maturation-related regulation of *Gsα* levels makes cells in the osteogenic lineage a natural target for the effects of mutations in the *Gsα* gene and may provide a clue as to why bone itself is affected in this somatic, mutation-dependent disease. (Am J Pathol 1997, 151:1587-1600)**

McCune-Albright syndrome (MAS) is a genetic, noninherited disease, defined by the triad of café-au-lait skin pigmentation, hyperfunctional endocrinopathies including precocious puberty, and polyostotic fibrous dysplasia.<sup>1,2</sup> The latter commonly causes deformity of affected skeletal segments, such as the typical shepherd's crook deformity of the femur, facial asymmetry, and/or bowing of tibia and ribs. Fibrous dysplasia of bone is commonly described and interpreted as the substitution of normal bone by an immature, disorganized fibro-chondro-osseous tissue, due to an overgrowth of primitive mesenchymal cells. However, the pathogenesis of fibrous dysplasia of bone has never been defined in more stringent, mechanistic terms. Activating missense mutations in the gene coding for the  $\alpha$ -subunit of Gs protein have been identified in MAS.<sup>3-5</sup> Substitution of either Cys or His for Arg at position 201 in the *Gsα* subunit leads to the loss of GTPase activity of *Gsα* and, as a consequence, to increased stimulation of adenyl cyclase and overproduction of cAMP. This somatic mutation has been demonstrated in a variety of tissues from patients with MAS, including bone,<sup>5-10</sup> and also in samples from the monostotic form of fibrous dysplasia.<sup>10-12</sup>

Supported in part by a Telethon Italia grant to P. Bianco (E.519).

Accepted for publication August 20, 1997.

Address reprint requests to Dr. Pamela Gehron Robey, Craniofacial and Skeletal Diseases Branch, National Institute of Dental Research, National Institutes of Health, Building 30 Room 106 MSC 4320, 9000 Rockville Pike, Bethesda, MD 20892.

M. Riminucci's current address is Department of Experimental Medicine, University of Rome "La Sapienza", Rome, Italy.

A. Shenker's current address is Department of Pediatrics, Northwestern University, Children's Memorial Hospital, 2300 Children's Plaza, Chicago, IL 60614.

**Table 1.** Summary of Patient Information

Patient	Age (years)	Sex	Site	Mutation	Reference
1	17	M	Femur, rib, vertebra (archival)	Cys	3 (case 2)
2	17	M	Site unknown (archival)	His	5 (case 3)
3	6	F	Occiput (archival)	Not determined	Determined from blood
4	8	F	Femur, maxilla (archival)		
5	10, 12	F	Maxilla (archival and new specimen)	His	Determined from blood
6	6, 11, 19	F	Femur (archival)	His	Determined from ovary

M, male; F, female.

The recognition of  $Gs\alpha$  mutations as the underlying genetic defect has clarified the pathophysiology of MAS to different extents in other organ systems. Overproduction of cAMP in endocrine tissues, for example, provides a straightforward clue to the endocrine hyperfunction that occurs in MAS. In contrast, the pathway by which overactivity of adenyl cyclase leads to the generation of fibrous dysplasia in bone is still unknown due to the complex cellular composition of bone tissue. Potential abnormalities in bone cell function brought about by these mutations must be recognized to dissect the mechanisms underlying the development of fibrous dysplasia.

In this study, we show that the entire spectrum of tissue changes observed in fibrous dysplasia of bone reflects a dysregulation of osteogenic cells. An expansion of the compartment of osteoprogenitor cells accounts for the development of fibrotic areas, whereas distinctive, newly identified abnormalities in the differentiated function of mature osteoblasts lead to deposition of abnormal bone. We also show that differentiation of mature osteoblasts from osteoprogenitor cells involves an up-regulation of  $Gs\alpha$  both in normal osteogenic tissues and in fibrous dysplasia and that changes observed in osteogenic cells *in situ* can be modeled *in vitro* as the effects of excess cAMP.

## Materials and Methods

### Patients

Six cases of MAS were the subject of this study and were collected as part of an Internal Review Board-approved National Institutes of Health protocol (protocol 96-DK-0055). A summary of relevant clinical data is given in Table 1. In two of the six cases, an activating mutation of the gene encoding the  $\alpha$ -subunit had been previously reported<sup>3,5</sup>; three were determined but not previously reported (Shenker, unpublished results), and in one patient, the mutation has not been determined (patient 3). The mutations were determined using polymerase chain reaction (PCR) and allele-specific oligonucleotides.<sup>3,5</sup>

### Tissues

Fresh surgical specimens of bone lesions were obtained from one patient who underwent corrective surgery (pa-

tient 5). Samples from this specimen were briefly fixed in 4% phosphate-buffered formaldehyde (overnight at 4°C), decalcified in 10% EDTA (pH 7.0), and embedded in paraffin or glycol methacrylate for histology. Archival paraffin blocks of decalcified tissue from the remaining five patients were also available. Sections were studied by both light and polarized light microscopy using a Zeiss Axiophot.

### Alkaline Phosphatase Activity

Undecalcified tissue was embedded in low-temperature glycol methacrylate as described previously<sup>13</sup> to preserve alkaline phosphatase activity. One-micron-thick sections were used for alkaline phosphatase activity using a simultaneous coupling azo dye method as described.<sup>13</sup>

### Immunohistochemical Detection of Bone Matrix Proteins and $Gs\alpha$

Rabbit antisera<sup>14</sup> against human versican (VSN; LF99), human decorin (DCN; LF30), human biglycan (BGN; LF15), human osteonectin (ON; HON), human osteopontin (OP; LF123), and human bone sialoprotein (BSP; LF6) were used at a dilution of 1:200 in 0.1% bovine serum albumin (BSA)/phosphate-buffered saline (PBS). All antisera were used in an indirect immunoperoxidase protocol. Briefly, deparaffinized sections (5  $\mu$ m thick) were exposed to 3% hydrogen peroxide for 30 minutes to inhibit endogenous peroxidase activity, washed in PBS, and incubated with a 1:10 dilution of normal goat serum for 30 minutes before exposure to primary antisera. Incubation time with primary antisera was for 2 hours at room temperature. After washing in 0.01% Triton X-100/PBS, the sections were incubated with a 1:100 dilution of a peroxidase-labeled, goat affinity-purified anti-rabbit IgG antibody (Kirkegaard and Perry, Rockville, MD) for 30 minutes. Immunoreactivity was revealed using the 3',3'-diaminobenzidine reaction.

Details of the production, characterization, and affinity purification of antibody RM/7, raised against human  $Gs\alpha$ , were previously published.<sup>15</sup> A second antibody (LF129) was generated against the synthetic peptide CDLLRCH-VLTS, corresponding to amino acids 196 to 205 of the

mutant (R201H) Gs $\alpha$ . The peptide was conjugated to LPH (hemocyanin from horseshoe crab; U.S. Biochemical, Cleveland, OH) by SulfoMBS (Pierce, Rockford, IL) and used for immunization in a previously described protocol.<sup>14</sup> Although raised against a mutant sequence, this antibody was determined to recognize normal Gs $\alpha$  as demonstrated by staining of Gs $\alpha$  in tissues from normal donors. To determine specificity of this staining pattern for Gs $\alpha$ , primary antibodies (LF129) were blocked with LPH-conjugated Gs $\alpha$  peptide (0.05  $\mu$ g/ $\mu$ l) at 4°C before incubation with tissue sections. Sections stained with an antibody against an irrelevant peptide (derived from serglycin, a mast cell proteoglycan) conjugated to LPH were negative. Similar blocking experiments were carried out with antibody RM/7 and the relevant peptide immunogen. By Western blotting, LF129 was found to be nonfunctional (as there was no reactivity with any proteins solubilized from cell layers of mature normal human trabecular bone cells), indicating that the epitope(s) are sensitive to the denaturing conditions used for gel electrophoresis. Both antisera were thus suited to assess the distribution of Gs $\alpha$  in normal osteogenic tissues and in fibrous dysplasia by immunohistochemistry and were used for this purpose. Sections of human fetal long bones from archival paraffin blocks were used to investigate the distribution of Gs $\alpha$  in normal subperiosteal bone formation, in which the normal progression of precursor osteogenic cells to mature osteoblasts is readily recognized.<sup>16,17</sup> Antibody RM/7 was used at a 1:50 dilution (30  $\mu$ g/ $\mu$ l), and antibody LF129 was used at a 1:200 dilution in 0.1% BSA/PBS.

#### *Expression of Gs $\alpha$ by Reverse Transcriptase (RT)-PCR/in Situ Hybridization*

A 300-bp sequence in the  $\alpha$ -subunit gene was chosen as the target for PCR amplification. A 5' oligonucleotide primer was designed based on the normal sequence of exon 8 of the Gs $\alpha$  gene, and the 3' reverse primer was complementary to a sequence in exon 11. The RT-PCR primer sequences used were as follows: 5'-GACCTGCTTCGCTGCCG and 5'-TCTTGCTTGTGAGGAACAG (reverse).

Specificity of the primer set for Gs $\alpha$  was verified by liquid-phase PCR followed by restriction enzyme digestion (BamHI) and agarose gel electrophoresis.

Tissues used for RT-PCR *in situ* were fixed in 4% buffered formaldehyde, decalcified in a 10% neutral solution of EDTA, and embedded in paraffin. After deparaffinization, sections (5  $\mu$ m) were digested with proteinase K (10  $\mu$ g/ml) for 15 minutes at 37°C. Reverse transcription of Gs $\alpha$  mRNA and amplification of cDNA were performed in the same reaction using the rTth DNA polymerase EZ buffer pack kit (Perkin Elmer, Norwalk, CT) according to the manufacturer's instructions. The reaction mixture contained 0.1 U/ml rTth DNA polymerase, 2.5 mmol/l Mn(OAc)<sub>2</sub>, 0.3 mmol/L each dNTP, and 1.5  $\mu$ mol/L each primer. Reverse transcription and amplification were performed in a single reaction, which was carried out at 60°C for 30 minutes (reverse transcription), followed by 20

cycles of denaturation at 94°C for 45 seconds, annealing of primer and template at 55°C for 15 seconds, and extension at 60°C for 60 seconds. Subsequently, the reaction was continued at 60°C for 5 minutes to ensure completeness of the last extension reaction. After the RT-PCR step, sections were hybridized with a 300-bp cDNA probe obtained by PCR from an osteoblastic library using the primers specific for Gs $\alpha$  and labeled with digoxigenin-dUTP for nonradioactive *in situ* hybridization. The hybridization was performed at 42°C in a mixture containing 50% formamide, 1X Denhardt's solution, 5% dextran sulfate, 200 mg/ml sheared and denatured salmon sperm DNA, 4X standard saline citrate (SSC), and 1 ng/ml probe. The cDNA probe was denatured by heating the sections at 95°C for 6 minutes. For digoxigenin immunodetection of the hybrids, alkaline-phosphatase-conjugated anti-digoxigenin (Fab') antibody was applied at a 1:500 dilution for 2 hours at room temperature. The sites of binding of the antibody were visualized by a chromogen solution containing 0.5 mg/ml nitroblue tetrazolium, 0.18 mg/ml X-phosphate, and 1 mmol/L levamisole. Specificity was determined by using sections in which either the enzyme or the primers had been omitted from the reaction step.

#### *In Situ Hybridization of Osteonectin mRNA*

A 243-bp ON cDNA probe was synthesized and labeled in a standard PCR reaction using the DIG-UNA labeling kit (Boehringer Mannheim, Indianapolis, IN). The following oligonucleotide primers were used: 5'-GTGGAAGTAGGAGAATTTGA-3' (forward, exon 4) and 5'-GCACTT-TGTGGCAAAGAAGT-3' (reverse, exon 6).

RT-PCR *in situ* hybridization was performed on formalin-fixed, paraffin-embedded tissue. After deparaffinization, sections were digested with 10  $\mu$ g/ml proteinase K (Boehringer Mannheim) for 15 minutes at 37°C, washed in 0.1 mol/L glycine in PBS, and hybridized with the cDNA probes at 42°C. The hybridization mixture contained 50% deionized formamide, 1X Denhardt's solution, 5% dextran sulfate, 200 mg/ml salmon sperm DNA, 4X SSC, and 1 ng/ $\mu$ l probe. The cDNA probe was denatured by heating the sections at 95°C for 6 minutes. After hybridization, the sections were washed once with 2X SSC and two times with 0.2X SSC for 20 minutes at 50°C. Immunodetection of the hybrids was performed as described above.

#### *Effects of cAMP on Osteogenic Cells in Vitro*

Rat fetal osteoblasts were isolated from calvariae of day 16 rat fetuses by sequential digestions of 20, 40, and 90 minutes with type IV collagenase (1 mg/ml; Sigma, St. Louis, MO) and trypsin (0.25%) at 37°C. Cells from the third digestion were plated in 35-mm culture dishes at a density of  $0.5 \times 10^4$  cells/dish and grown to confluence in Dulbecco's modified minimal essential medium supplemented with 10% fetal calf serum, 2 mmol/L glutamine, 100 U/ml penicillin, and 100 mg/ml streptomycin (Sigma Chemical Co., St. Louis, MO), at 37°C in a 5% CO<sub>2</sub>

atmosphere. First-passage cells were seeded onto coverslips and, when confluent, incubated in serum-free medium for 16 hours before use.

Normal human trabecular bone cells were prepared from pieces of normal bone under IRB-approved procedures as described previously.<sup>18</sup> Briefly, fragments of trabecular bone were minced to the consistency of sand and treated with bacterial collagenase (250 U/ml collagenase P; Boehringer Mannheim) to remove soft tissue and associated cells. The collagenase-treated fragments were placed in low-calcium nutrient growth medium containing a 50:50 mixture of Dulbecco's modified minimal essential medium/HF12K, with 10% fetal bovine serum, glutamine, penicillin, and streptomycin. Medium was replaced three times per week. Cells grew out from the fragments after approximately 1 to 2 weeks and became confluent within 4 to 6 weeks.

When confluent, both rat and human cultures were incubated in serum-free medium for 16 hours before use. Subsequently, they were treated with 1 mmol/L dibutyryl cyclic AMP (db-cAMP) for 2 hours. Control cultures were left untreated in serum-free medium.

## Results

### Osteogenic Nature of Fibroblastic Cells in Fibrotic Areas

To characterize the phenotypic properties of fibroblast-like cells in fibrotic areas of fibrous dysplasia, we investigated the expression of known histological markers of osteogenic cell differentiation. One-micron-thick glycol methacrylate sections cut from tissue blocks processed at low temperature were used to assess the distribution of alkaline phosphatase activity, a hallmark of cellular commitment to the osteoblastic lineage.<sup>17,19</sup> Cells located within the fibrous tissue as well as cells associated with bone surfaces exhibited distinct plasma-membrane-associated activity (Figure 1A). The cells within fibrous tissue were noted for their branched, stellate morphology, clearly outlined by the reaction product. Comparable paraffin sections were used to assess the expression, within the fibrous tissue, of bone proteins expressed during osteogenic cell differentiation and maturation. A felt-like network of immunoreactive structures, interpretable as cell processes and/or extracellular matrix structures, was revealed by immunolabeling for the large proteoglycan VSN and the small proteoglycans DCN and BGN (BGN not shown; Figure 1, B and C). Fibroblastic cells consistently displayed intracellular labeling for ON (Figure 1D) and occasional labeling for OPN (Figure 1E). They were consistently negative for the late marker of osteogenic cell maturation, BSP (Figure 1F). These data

indicate that fibroblast-like cells in fibrotic areas of fibrous dysplasia, like committed osteogenic precursors and unlike soft tissue fibroblasts, exhibit high levels of cell-surface-associated alkaline phosphatase activity. Bone-related proteins associated with early stages of osteogenic cell maturation (VSN, DCN, BGN, and ON), are also expressed in these cells, whereas bone-related proteins associated with late stages of osteoblast maturation (particularly BSP) are not expressed. These data indicate that fibroblast-like cells of fibrous dysplasia share some phenotypic features with osteoprogenitor cells of normal osteogenic tissues.

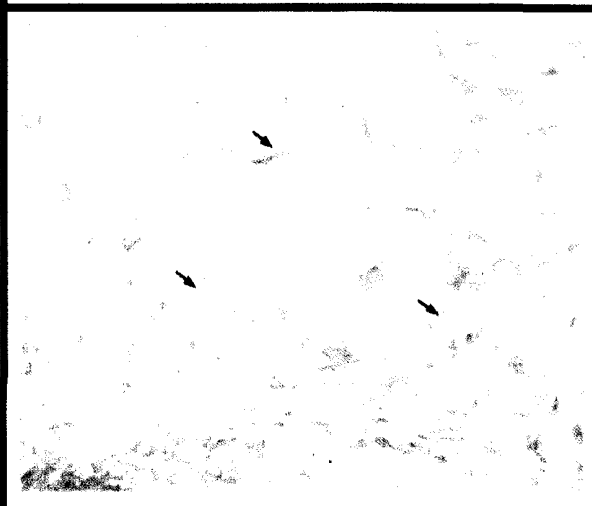
### Structural and Cellular Changes at Bone Formation Sites

It is commonly reported that bone trabeculae found in fibrous dysplastic lesions consist characteristically of woven bone.<sup>20</sup> This type of bone exhibits a haphazard orientation of loosely textured collagen fibers and is usually found at sites of *de novo* bone formation in normal osteogenesis. In contrast, normal human secondary (ie, after remodeling) bone is characterized by a lamellar organization of collagen fibers.<sup>21</sup> By studying all of our samples using polarized light microscopy, we found that bone trabeculae found within fibrous dysplasia were in fact heterogeneous in structure. Although typically made of woven bone in some areas, bone trabeculae found within the fibrotic tissue were clearly lamellar in others and merged with normal lamellar (compact or trabecular) bone toward the edges of the lesions. These lamellar trabeculae usually showed evidence of extensive bone resorption. Polarized light microscopy thus provided an easy means for distinguishing normal, pre-existing lamellar bone trabeculae (Figure 2A), which became partially resorbed and then entrapped within fibrous dysplasia, from abnormal trabeculae formed *de novo* within fibrous dysplastic tissue and representing true lesional bone (completely woven in structure; Figure 2B).

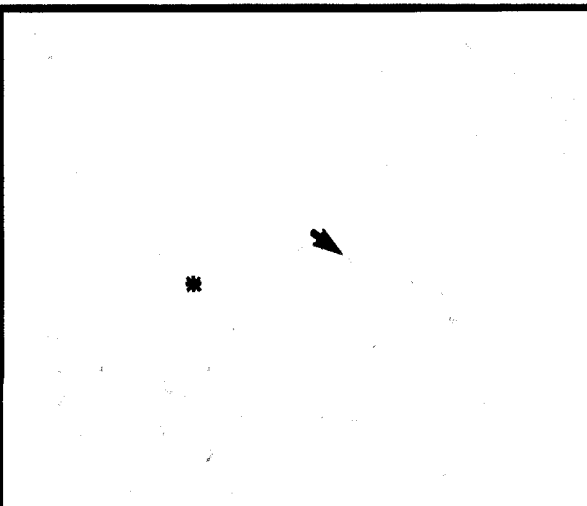
Further observation of the newly formed, lesional bone revealed additional characteristic changes in bone structure and in bone cell morphology (Figure 3). As best demonstrated by either polarized light or differential interference contrast (DIC) microscopy, the deposition of bone collagen bundles was noted to occur perpendicular to the forming bone surface instead of parallel as usually observed in both normal woven and lamellar bone. This resulted in a combed appearance of the forming bone surfaces (Figure 3A). A prominent retraction of osteoblast cell bodies, sometimes resulting in pseudo-lacunar spaces lining the

**Figure 1.** Expression of bone-related proteins by fibroblastic cells within dysplastic lesions of MAS. Cells associated with bone surfaces (not shown) as well as retracted cells and cells within fibrous tissue exhibit distinct plasma membrane-associated alkaline phosphatase activity (A). The cells within fibrous tissue were noted for their branched, stellate morphology, clearly outlined by the reaction product (small arrows). As revealed by immunolocalization on comparable paraffin sections, these cells (large arrows) as well as a felt-like network of immunoreactive structures, interpretable as cell processes and/or extracellular matrix structures (asterisk), were revealed when stained for the proteoglycans (VSN; B) and decorin (DCN; C). Staining of cell bodies only (large arrows) was observed when comparable sections were stained for ON (D) and to some extent for OPN (E). Neither cells nor matrix were found to stain for BSP (F). Glycol methacrylate section (A) and paraffin sections viewed with Nomarski optics (B); magnification,  $\times 125$ .

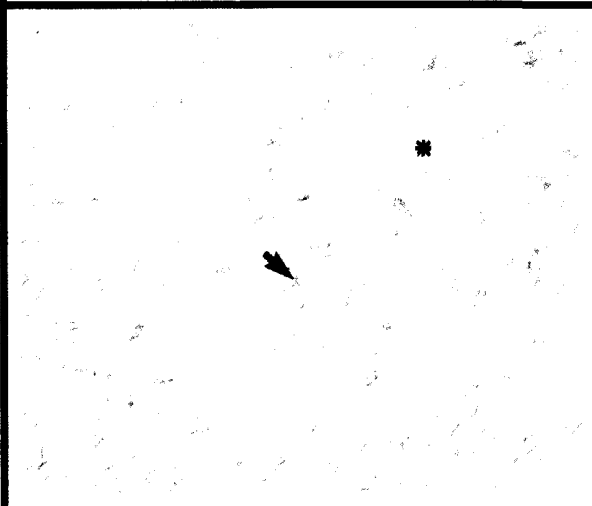
### CHARACTERIZATION OF FIBROBLASTIC CELLS



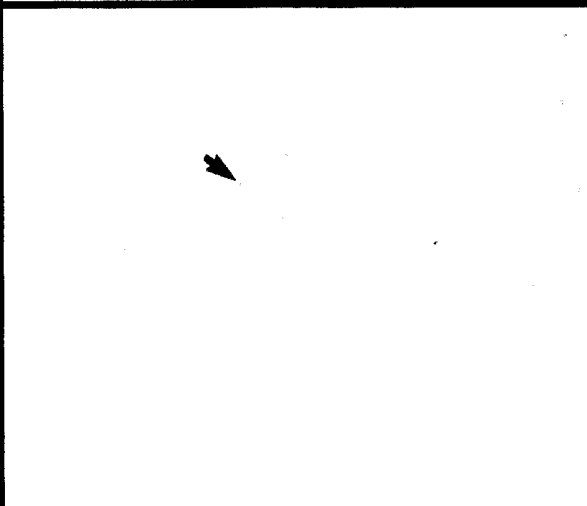
A. ALP



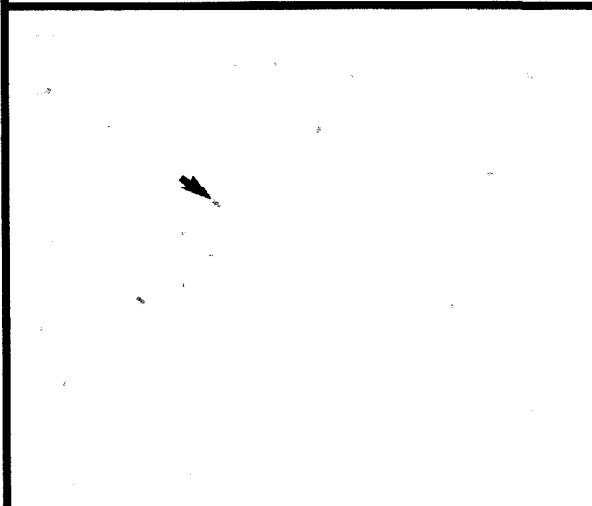
B. VSN



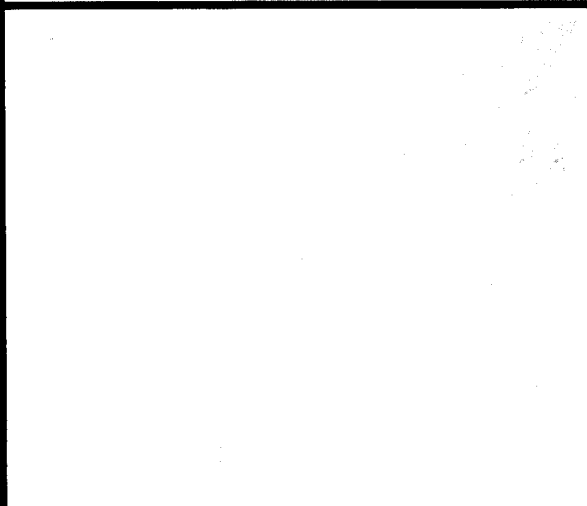
C. DCN



D. ON



E. OPN



F. BSP

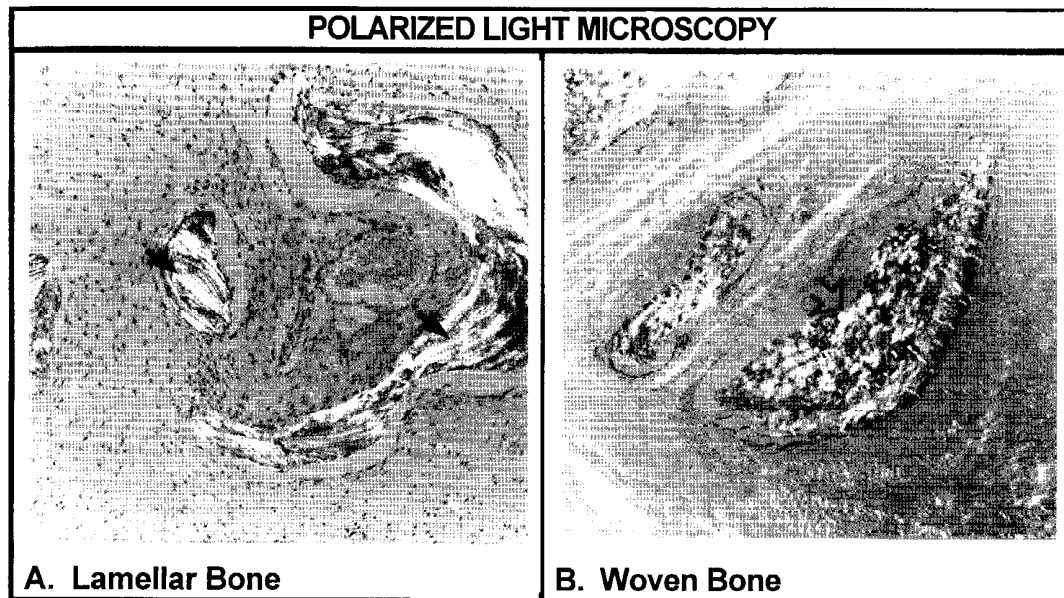


**Figure 2.** Polarized light microscopy of typical fibrous dysplasia lesions. Some trabeculae consisted entirely of typical lamellar bone (A), whereas others consisted of woven bone (B). The former represent residual normal bone, whereas the latter represent bone formed *de novo* within the lesion. Magnification,  $\times 70$ .

trabecular surfaces was associated with this pattern of collagen deposition (Figure 3B). An additional abnormal feature of bone formation sites was given by the occurrence of excess osteogenic cells crowding the bone surfaces, resulting in the formation of a hypercellular bone matrix with unusually large osteocytic lacu-

nae. These were often seen to accommodate several osteocytes each and to outline a maze of spaces running through a trabecula (hyperosteocytic bone; Figure 3C). From these data, we concluded that distinct structural and cellular changes are found in lesional bone formation sites in fibrous dysplasia.

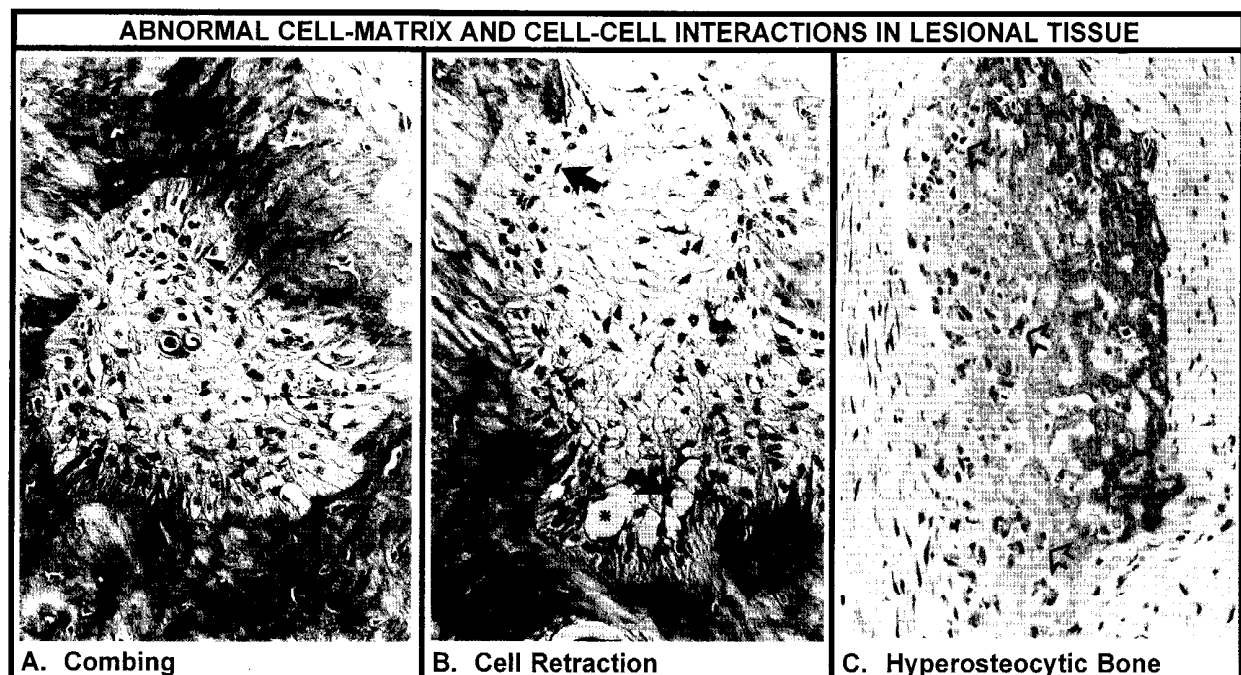


**Figure 3.** Unique histological features of osteoblastic cells associated with *de novo* bone formation. Distinct changes in osteoblast shape, number, mutual organization, and association with the extracellular matrix were a general finding in the newly formed, woven, lesional bone from all patients. Deposition of collagen bundles was oriented perpendicular to a forming surface (small arrows) instead of co-linear (a pattern we define as combed to note its peculiarity with respect to woven bone; A). A prominent retraction of osteoblast cell body was apparent (large arrows), sometimes resulting in pseudo-lacunar spaces (asterisk) lining the trabecular surfaces (B). The formation of unusually large osteocytic lacunae each accommodating several cells (open arrows) and outlining a maze of spaces running through a trabecula (hyperosteocytic bone) was also a distinguishing feature (C). Magnification,  $\times 125$  (A and B) and  $\times 100$  (C).

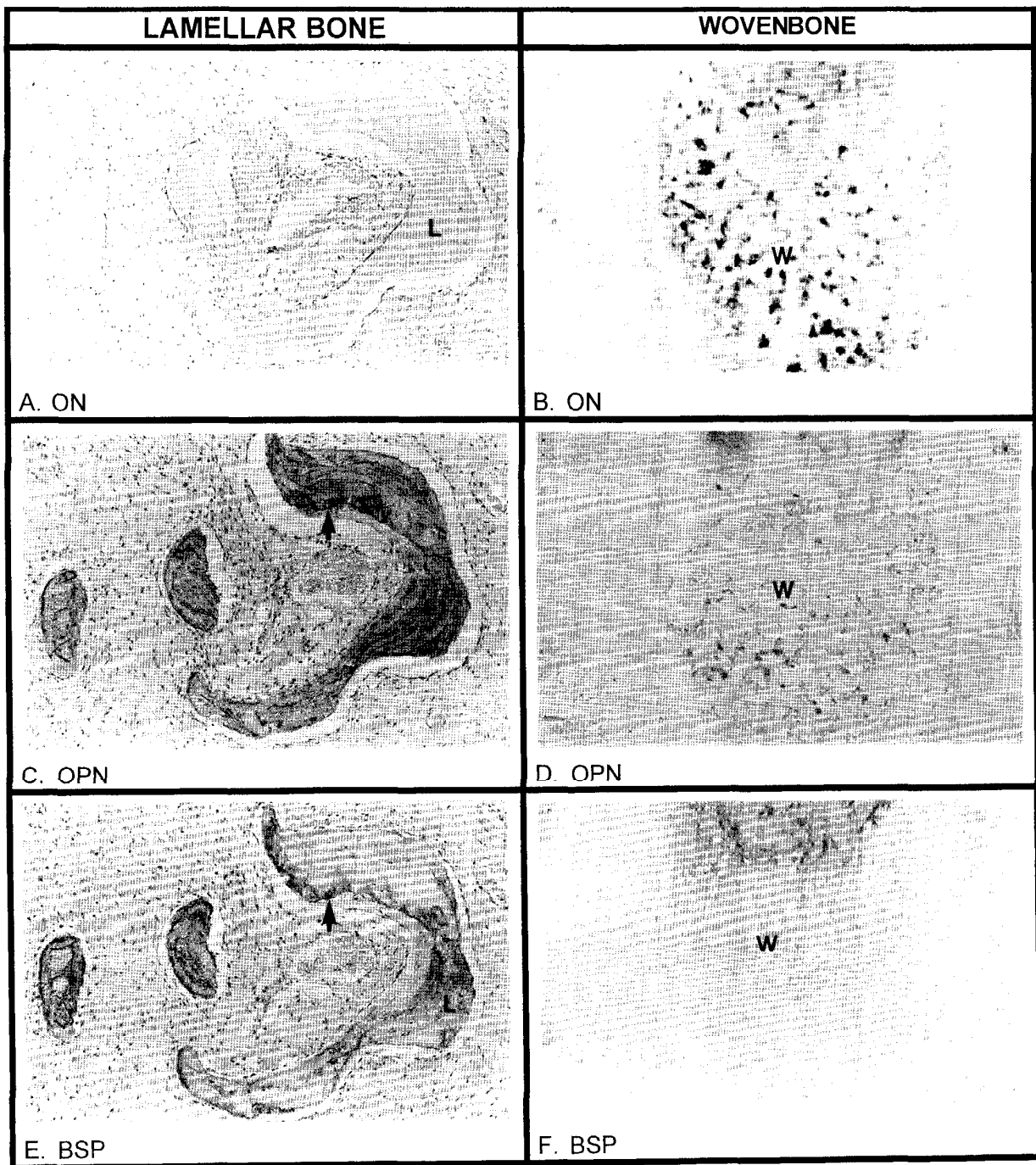


**Figure 4.** Expression of bone matrix proteins in normal lamellar and fibrous dysplastic woven bone. The profile of matrix protein immunoreactivity seen in pre-existing, lamellar (L) as compared with woven, newly formed bone (W) in fibrous dysplasia lesions is different. Immunoreactivity for ON was virtually absent from lamellar bone (A) but prominent throughout the newly formed woven bone and associated osteogenic cells in the lesional tissue (B). Immunoreactivity for OPN was prominent in osteoblastic cells and in lamellar bone (C) but was barely detectable both in the cells and in the matrix in lesional woven bone (D). In a similar fashion, BSP was also prominent in osteoblastic cells and in cement lines in lamellar bone (E) but undetectable in lesional woven bone (F). Note reinforced labeling for OPN and BSP at cement lines in lamellar bone (C and E, arrowheads). Magnification,  $\times 70$  (A, C, and E) and  $\times 125$  (B, D, and F).

### *Expression of Bone Matrix Proteins in Fibrous Dysplasia*

We also investigated potential differences in the bone matrix composition of normal, lamellar bone and lesional

trabeculae within MAS tissues. The bone matrix in lamellar entrapped bone was devoid of immunoreactivity for ON but strongly immunoreactive for OPN and less uniformly yet distinctly immunoreactive for BSP (Figure 4, left column). OPN and BSP were specifically enriched in the



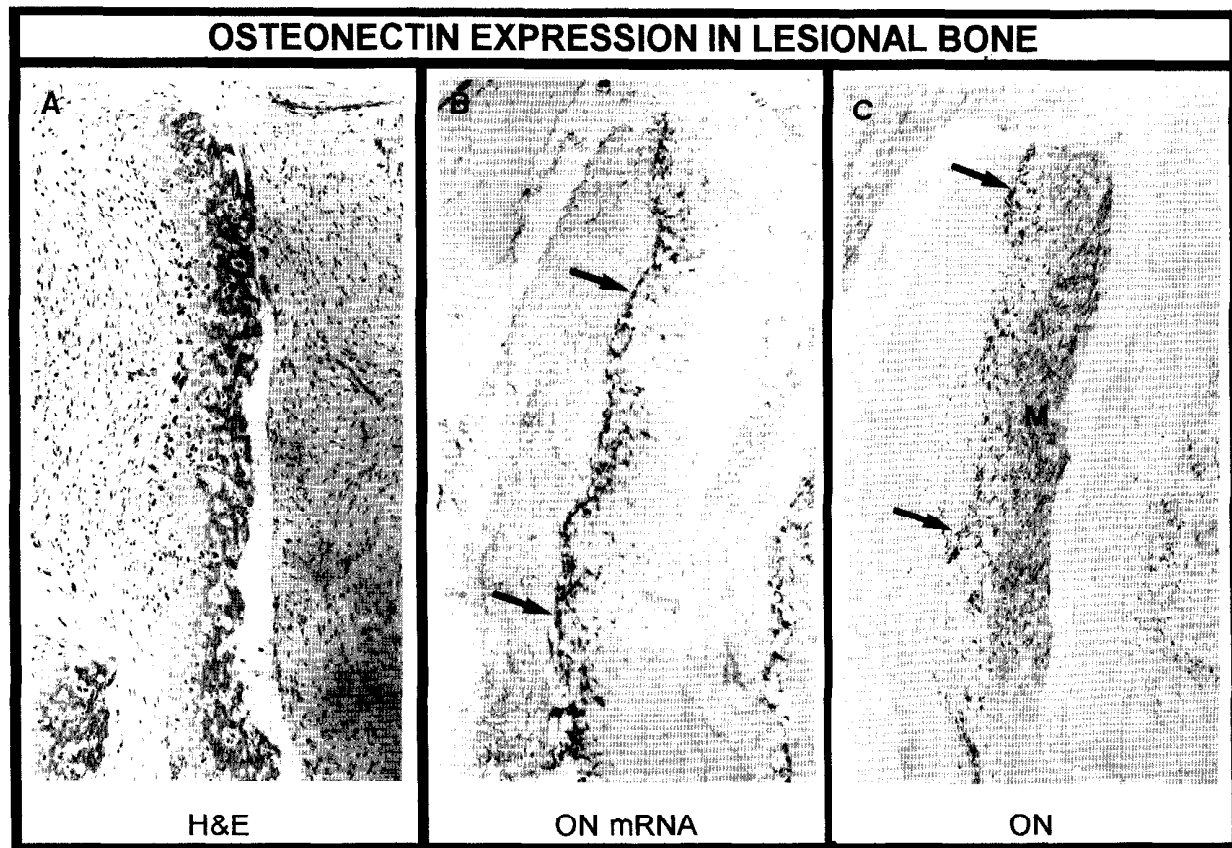


**Figure 5.** Demonstration of endogenous production of ON. Immunolocalization of ON indicated that newly formed woven bone in dysplastic lesions was rich in ON. As ON can be adsorbed from other sources, endogenous synthesis was demonstrated by localizing mRNA for ON using a specific cDNA probe. Serial sections of a typical lesion (A) were used for analysis. The probe hybridized strongly with mRNA in osteoblastic cells (arrows) in the process of depositing woven bone within the lesional tissue (B). The cellular pattern is identical to the pattern observed by immunolocalization of ON (C), which also showed the deposition of ON in bone matrix (M). Magnification,  $\times 70$ .

cement lines marking previous episodes of bone remodeling. This pattern was identical to the one observed in normal compact and trabecular bone within nonlesional areas in our tissue samples and in bone from unaffected patients (not shown). In comparison, the bone matrix seen in *de novo*, all-woven bone was prominently immunoreactive for ON and barely, if at all, immunoreactive for OPN and BSP (Figure 4, right column). The cellular pattern of distribution for the same proteins matched the profile of matrix immunoreactivity with extremely prominent staining of ON and weak or absent staining for OPN and BSP. The cellular pattern of distribution of VSN in abnormal bone mimicked closely the one observed with antisera for ON. Unlike ON, however, VSN was not localized within bone matrix (not shown). This cellular pattern of staining is similar but not identical to the pattern found in normal woven bone, where VSN and ON are found to be expressed at high levels. However, in normal woven bone, OPN and BSP are also found at high levels.<sup>16</sup> Consequently, the woven bone found in the lesion does not contain the normal complement of bone matrix proteins.

To further substantiate the findings that the high levels of ON protein in lesional bone-forming cells was due to endogenous synthesis, sections were used for *in situ*

hybridization experiments using an ON cDNA probe. High levels of ON mRNA (Figure 5B) were found to match the strong intracellular labeling of ON protein (Figure 5C). Both ON mRNA and protein were prominent at sites of cellular retraction.

#### *Expression of Gs $\alpha$ in Normal and Fibrous Dysplastic Tissues*

We next investigated the distribution of Gs $\alpha$  in normal osteogenic tissues and fibrous dysplasia to gain insight into where altered Gs $\alpha$  activity may exert its influence in the bone microenvironment (Figure 6). Sections of human fetal long bones were immunostained using two different sequence-specific peptide antisera. In such sections, sites of subperiosteal bone formation provide a histological model of osteogenic cell differentiation, in which fibroblasts, pre-osteoblasts, and mature osteoblasts are found in a spatially defined sequence.<sup>16,17</sup> A very strong signal was detected in mature osteoblasts associated with forming bone surfaces and early osteocytes. Pre-osteoblastic and fibroblastic cells residing next to the mature osteoblasts in the periosteum displayed significantly lower but detectable levels of signal. A similar



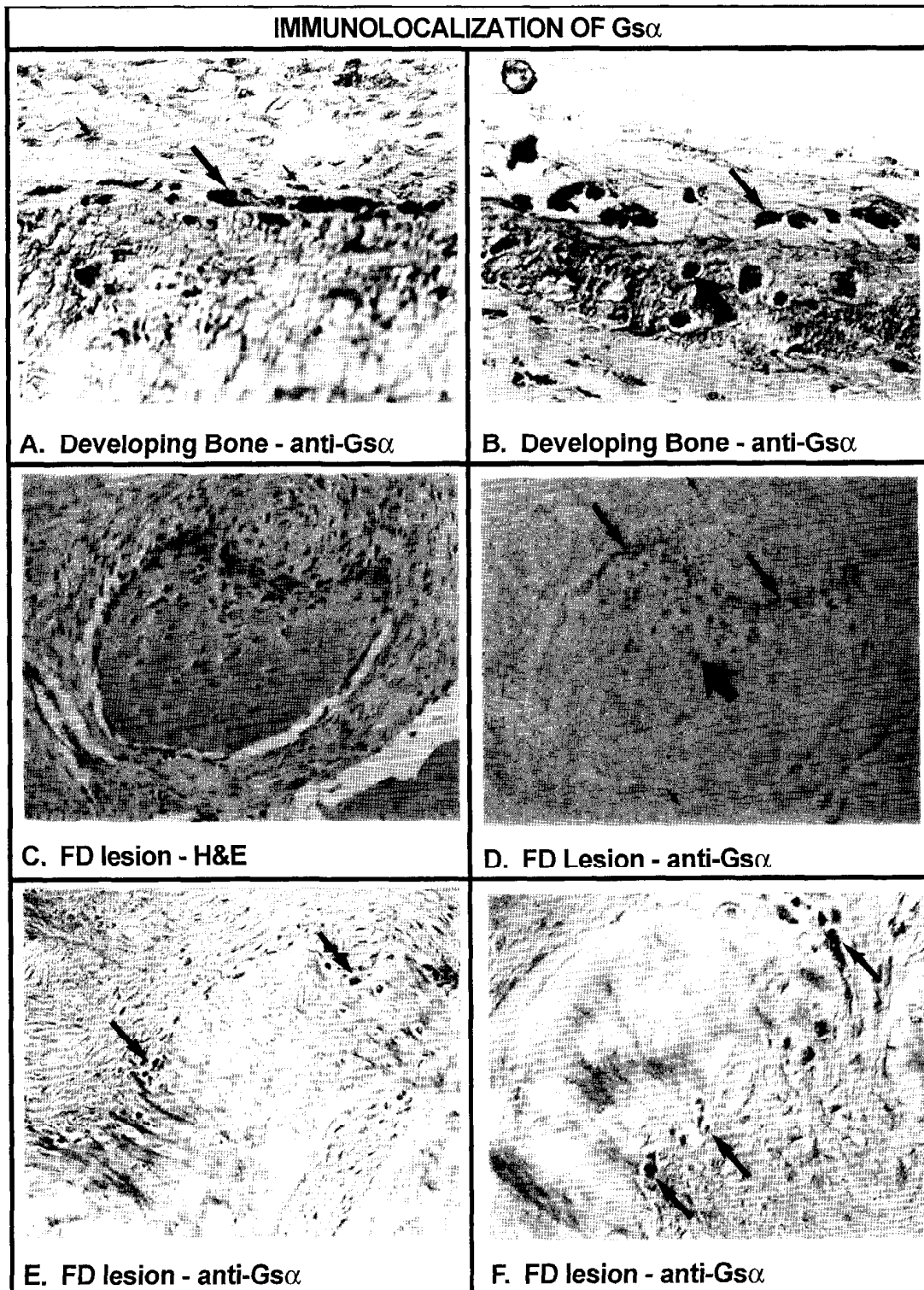


**Figure 6.** Localization of Gs $\alpha$  expression by immunohistochemistry. In areas of *de novo* bone formation in developing human subperiosteal bone (A and B), the expression of Gs $\alpha$  was determined using an antibody raised against a synthetic peptide (see Materials and Methods). This antibody recognizes both normal and mutated Gs $\alpha$ . Osteoblasts (medium arrows) on the newly formed bone are intensely stained whereas pre-osteoblastic cells (small arrows) show a low level of reactivity. In lesional tissue (C), a similar pattern is observed. Fibrous cells displayed a low level of reactivity (small arrows), and the osteoblastic layer (medium arrows) and newly embedded osteocytes (large arrow) were found to be highly reactive (D). Immunoreactive osteoblasts were also noted in areas of collagen combed and cell retraction (E and F). H&E (C); Nomarski optics (B, E, and F); magnification,  $\times 175$  (B),  $\times 125$  (F), and  $\times 70$  (C, D, and E).

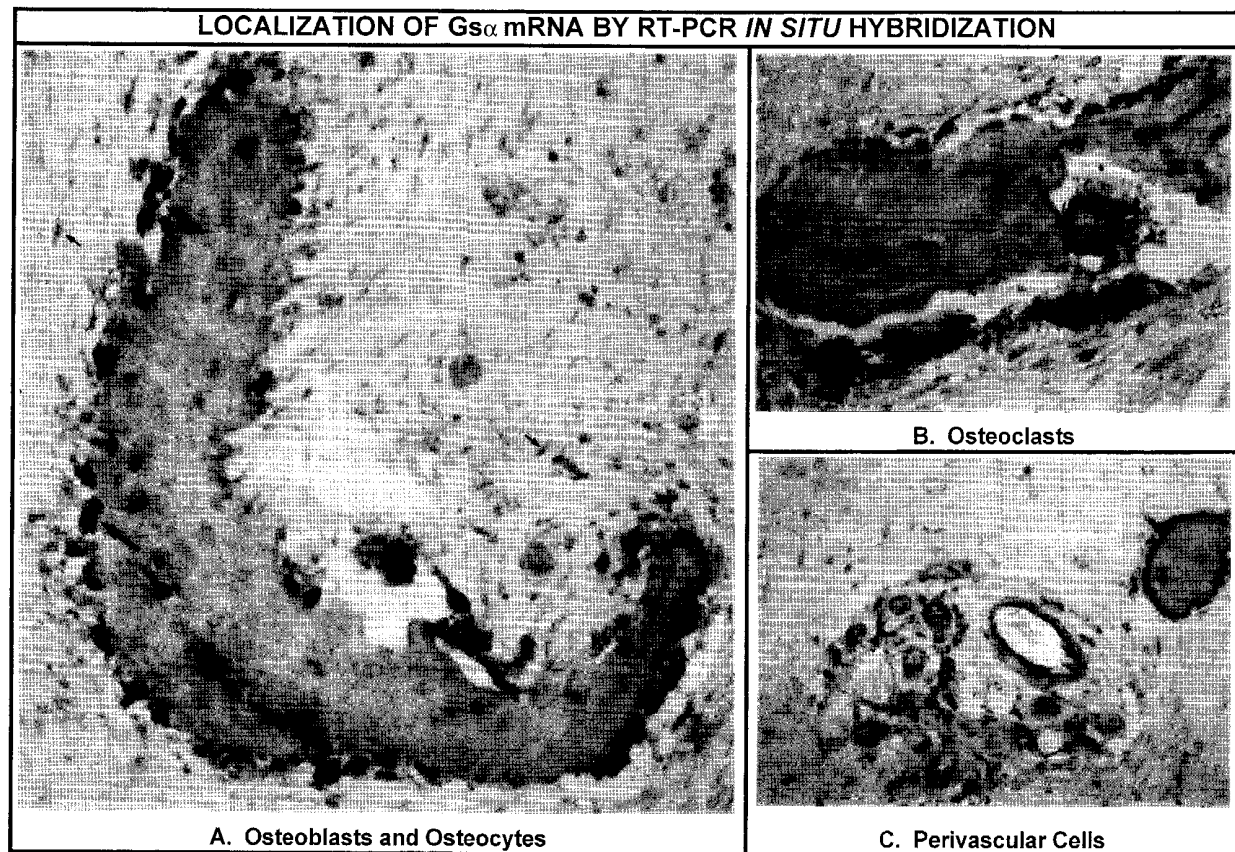


**Figure 7.** Localization of  $Gs\alpha$  mRNA by RT-PCR *in situ* hybridization. Expression of  $Gs\alpha$  mRNA was determined by RT-PCR *in situ* hybridization as described in Materials and Methods. Levels of signal for  $Gs\alpha$  mRNA were not uniform in individual tissue components. Low levels were detected in fibroblastic cells (small arrows), and high levels were detected in osteoblasts (medium arrows) and early osteocytes (large arrows) (A). Osteoclasts (B) and cells associated with the adventitia of blood vessels (C) were also found to express high levels of  $Gs\alpha$  mRNA. No reaction was observed in control sections when either the primers or the enzyme were omitted from the reaction mixture (not shown). Magnification,  $\times 250$  (A),  $\times 125$  (B), and  $\times 100$  (C).

pattern of labeling was observed in sections of fibrous dysplastic lesions. High levels of signal were also detected in osteoblastic cells associated with the surface of abnormal bone trabeculae and in early osteocytes, and low levels were found in the fibroblast-like cells occupying the fibrotic areas. In addition, osteoclastic cells and cells associated with the walls of small arteries were also found to contain  $Gs\alpha$  in both normal and abnormal tissues (not shown). No signal was detected in control sections incubated with antisera preadsorbed with the relevant peptide. Identical results were observed in sections in which  $Gs\alpha$  mRNA was detected by RT-PCR *in situ* hybridization (Figure 7), again with high levels detected in osteoblasts, osteocytes, osteoclasts, and cells of the adventitia of small blood vessels. We concluded that, within sites of bone formation, expression and biosynthesis of  $Gs\alpha$  are characteristically higher in mature osteogenic cells (osteoblasts and early osteocytes) compared with fibroblast-like cells, including osteogenic cells in a

pre-osteoblastic stage of differentiation. These data suggest that  $Gs\alpha$  is highly up-regulated during the transition of osteogenic cells from a pre-osteoblastic to a fully mature osteoblastic phenotype.

#### *Effect of cAMP on Osteoblastic Cell Shape in Culture*

As overactivity of adenylyl cyclase is a known consequence of activating missense mutations in the  $Gs\alpha$  gene, we hypothesized that the altered cell shape of bone-forming cells observed in the fibrous dysplasia lesions (Figure 8A) might directly reflect increased intracellular levels of cAMP. Based on earlier evidence that parathyroid hormone (PTH) or other stimulators of cAMP formation can induce shape changes in osteoblastic cells in rodent osteoblastic cell culture models,<sup>22</sup> the effects of db-cAMP on osteoblastic cultures were studied. Addition

**Figure 8.** Comparison of cell retraction in fibrous dysplastic lesions *in vivo* to cell retraction induced by addition of cAMP to osteoblastic cells *in vitro*. Cellular retraction of osteoblastic cells in fibrous dysplastic lesions is a characteristic morphological feature (A) that may be linked to excess endogenously produced cAMP. Similar changes in cell morphology were noted when confluent monolayers of rat calvarial cells (RCC) and primary human adult trabecular bone cells (NHTB) were incubated overnight in serum-free conditions and subsequently treated with 1 mmol/L db-cAMP (B and D). On administration of db-cAMP in the absence of serum, both human and rat osteoblastic cells assumed a retracted, stellate shape compared with control (C). The retraction was completely reversible by removing the excess cAMP and further incubation. These changes were verified in three separate experiments. Magnification,  $\times 125$ .

**CELL RETRACTION *IN VIVO* AND *IN VITRO***



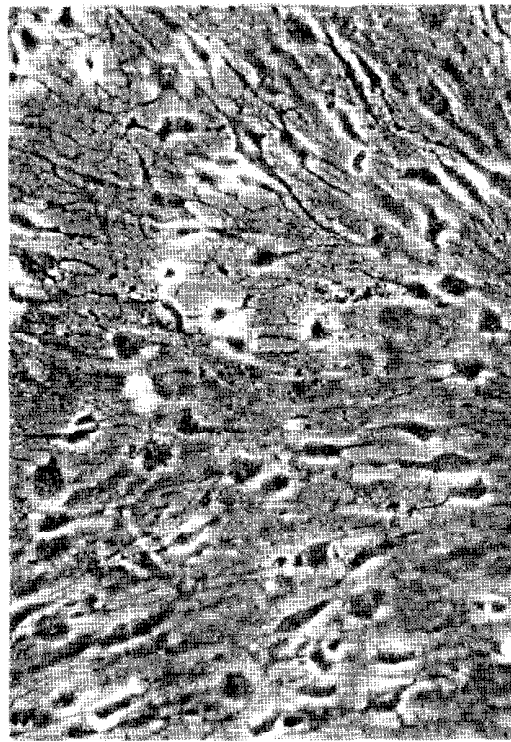
**A.** Fibrous Dysplastic Lesion



**B.** RCC + 1 mM db-cAMP



**C.** NHTB Control



**D.** NHTB + 1 mM db-cAMP

of db-cAMP caused a dramatic effect on rat calvarial cells and normal human trabecular bone cells (Figure 8, B and D). On administration of cAMP in the absence of serum, cells assumed a retracted, stellate shape within 30 minutes compared with control (Figure 8C). This effect was reversible, and cells resumed the original shape and spreading on removal of the excess cAMP. Excess cAMP in cultures of rat and human osteoblastic cells produced a transient cell shape change that mimicked the shape of osteoblastic cells observed *in situ* in MAS fibrous dysplasia.

## Discussion

Contrary to the general description in many textbooks that fibrous dysplasia of bone represents an overgrowth of nondescript fibrotic tissue with a secondary phenomenon of bony metaplasia, we show here that the development of fibrous dysplasia of bone within the MAS reflects a complex derangement in the function of cells in the osteogenic lineage, of which we have defined several aspects, along with potential links to adenyl cyclase overactivity.

The fibrous component of the dysplastic lesion is in fact composed of cells with features of early pre-osteoblastic, rather than fibroblastic, cells. As such, it is to be distinguished from common fibrosis. We have shown that cells populating the fibrotic areas of fibrous dysplasia express alkaline phosphatase activity, which indicates their relationship to the osteogenic lineage (of which alkaline phosphatase is the best known and earliest marker; reviewed in Ref. 21) and their divergence from nonosteogenic fibroblasts. In addition to alkaline phosphatase activity, normal osteoprogenitor cells express certain proteins found in bone matrix, including the large proteoglycan VSN,<sup>23</sup> the two small proteoglycans DCN and BGN,<sup>24</sup> and ON<sup>25</sup> but do not express the late marker of osteoblast differentiation, BSP.<sup>17</sup> Unlike mature osteoblasts, osteoprogenitor cells proliferate *in vivo*.<sup>18,29</sup> Recent data indicating increased expression of c-fos<sup>8</sup> and cell proliferation<sup>10</sup> in heterogeneous cultures of cells grown from fibrous dysplasia of bone may thus directly reflect the local enrichment in osteoprogenitor cells (the fibrosis) in the parent, lesional tissue.

Deposition of bone within fibrous dysplasia does not represent metaplasia of fibrous tissue. As the fibrous tissue itself consists of osteogenic cells, invoking a shift in phenotype of fibroblasts comprising the fibrotic areas is unnecessary. Besides, metaplasia is usually taken as an explanation for the lack of morphologically recognizable osteoblasts along the surfaces of bone trabeculae found within fibrotic lesions. We have shown here that only some of such trabeculae do in fact represent deposition of lesional bone, whereas others are remnants of pre-existing, normal bony structures, recognized by their mature lamellar structure. Unlike these residual, nonlesional structures, true lesional bone is the product of recognizable abnormal osteoblasts, which differentiate within the fibrous dysplastic tissue. These cells deposit an abnor-

mal bone matrix with distinct structural features and chemical composition.

With respect to the structural features, bone-forming cells associated with the deposition of new, lesional bone display retracted cell bodies and deposit abnormally oriented collagen bundles onto forming surfaces (combining). As collagen orientation in bone reflects the orientation of the cell body of osteoblasts,<sup>21</sup> deposition of collagen bundles running perpendicular to the forming surface is easily correlated to the retraction of the osteoblast cell body. This pattern of collagen and osteoblast orientation, consistently observed in all samples of fibrous dysplasia, is not known to recur in other bone diseases, and it is not observed at zones of transition between mineralized and soft tissues under normal conditions. Interestingly, however, a somewhat similar pattern of collagen orientation (so-called Sharpey fiber bone) is known to become established at certain anatomical sites (insertion of tendons and periodontal ligament and cranial sutures), where specific tensile strain patterns are reflected in collagen orientation perpendicular to the bone surfaces.

As to the biochemical composition, the enrichment of ON and the low levels of OPN and BSP distinguish lesional bone from pre-existing lamellar trabeculae. The matrix composition of lesional bone reflects levels of protein expression in the associated osteoblasts, as shown here by immunostaining and *in situ* hybridization data. Overall, the profile of matrix protein expression found in osteoblasts involved with the *de novo* deposition of lesional bone differs from the profile seen in normal *de novo* bone formation. Under normal conditions, *de novo* bone formation is in fact associated with high levels of VSN and ON, but also, and characteristically, with OPN and BSP.<sup>26,27</sup> VSN and ON are reported to be associated with loss of cell-matrix adhesion and changes in cell shape, respectively, and are sometimes referred to as anti-adhesins. In contrast, OPN and BSP are known ligands of bone cell-surface-associated integrins and effectively promote cell adhesion in *in vitro* models.<sup>28,29</sup> Therefore, the composition of the matrix produced by abnormal osteoblasts is shifted toward molecules favoring cell shape changes and opposing cell adhesion. Current data indicate that Gs $\alpha$  mutations are found in bone lesions and in cells grown in culture from bone lesions of patients with MAS.<sup>6-10</sup> We have for the first time localized Gs $\alpha$  and its cognate mRNA in osteogenic tissues and shown that mature osteoblasts exhibit distinctly higher levels of their expression compared with osteogenic precursor cells. This suggests that the terminal maturation and the differentiated function of osteogenic cells (that is, the development of mature osteoblasts and the deposition of a normal mineralizing bone matrix) are critically associated with Gs $\alpha$  function and its regulated expression. In itself, this observation may provide a clue as to why bone is particularly susceptible to pathological changes related to Gs $\alpha$  mutations.

A comparison of normal and fibrous dysplastic tissues shows that this pattern of expression of Gs $\alpha$  is retained in fibrous dysplasia, where low levels of Gs $\alpha$  are found in osteogenic precursor cells of fibrotic areas and high

levels are found in mature, abnormal osteoblasts. Our data do not provide direct evidence, in histological terms, for the precise identity and frequency of cell types bearing the activating  $Gs\alpha$  mutation in bone lesions. However, it is reasonable to postulate that an up-regulation of the expression of mutant  $Gs\alpha$  in mature osteoblasts would result in a large excess of cAMP. All of the structural and biochemical abnormalities that we observed in mature bone-forming cells in fibrous dysplasia can in fact be related to the effects of excess cAMP.

The distinctive retraction of the osteoblast cell body observed *in situ* was directly modeled in our experiments using normal human osteoblastic cells and db-cAMP. In these experiments, cell retraction was observed within 30 minutes after the addition db-cAMP and was transient and spontaneously reversible. This cellular retraction is accompanied by internalization of focal adhesions and a distinct pattern of rearrangement of cytoskeletal elements as visualized by confocal microscopy (Riminucci and Bianco, manuscript in preparation). In a now classical hypothesis derived from organ culture studies on the effects of PTH on osteogenic cells, PTH-induced cell retraction was postulated to occur normally before the initiation of bone remodeling.<sup>30</sup> However, an *in vivo* correlate of this phenomenon has never been observed in normal human bone, probably because of the elusiveness of its cytological detail in tissue sections and as a result of its transient nature. In contrast, retracted osteogenic cells were reported in endosteal surfaces in human hyperparathyroidism,<sup>31</sup> in which excess cAMP is an expected consequence of inappropriate hormonal levels. In MAS, overactivity of adenyl cyclase in the same signal transduction pathway is the consequence of  $Gs\alpha$  mutations in the absence of receptor-ligand interaction. This suggests that overactivity of the same signal transduction pathway in both hyperparathyroidism and MAS is conditional to detection of the cell retraction phenomenon *in situ*, as a reflection of either its increased frequency or its prolonged temporal dimension, or both.

The cellular response to stable elevated levels of cAMP as found in cells bearing the  $Gs\alpha$  mutation may in turn be the increased synthesis of such anti-adhesive proteins as VSN and ON in the absence of the adhesive proteins OPN and BSP, as observed here. There are multiple cAMP response elements in the VSN promoter and the ON promoter,<sup>32</sup> as well as a half cAMP response element in the BSP promoter.<sup>33</sup> The major protein induced by db-cAMP in F9 teratocarcinoma cells is ON, and interestingly, when these cells overexpress ON, they exhibit a shift in cell shape and a reduced adhesiveness.<sup>34</sup> On the other hand, PTH, which stimulates high levels of intracellular cAMP, decreases the level of OPN mRNA in osteosarcoma cells.<sup>35</sup> Taken together, our *in vitro* findings and our *in situ* data on the morphological and biochemical phenotype of osteoblast in fibrous dysplasia suggest that both early and late responses to increased cAMP contribute to establish abnormal patterns of osteoblast-matrix interaction, which may be a critical factor leading to deposition of abnormal bone in fibrous dysplasia.

In summary, our data provide a potential mechanism for the development of fibrous dysplasia as a result of  $Gs\alpha$  mutation in cells of the osteogenic lineage. Development of mature osteoblasts from committed precursor cells brings about a critical increase in levels of  $Gs\alpha$ . This results, in the presence of mutated  $Gs\alpha$ , in excess formation of cAMP, reflected in characteristic cAMP-induced changes in osteoblast shape and interaction with the extracellular matrix. This interferes with the assembly of a structurally normal bone matrix, and peculiar textures of the collagenous matrix are generated. Long-term effects of cAMP on mature osteoblasts dysregulate the expression of several bone matrix proteins, resulting in a matrix with distinct stoichiometry, in itself conducive of loosened cell-matrix interaction. Ineffective deposition of bone ensues, resulting in thin, abnormal, bone trabeculae associated with an expanded population of pre-osteogenic cells. Malfunction of mature osteoblasts might disrupt a homeostatic balance between immature (pre-osteoblastic) and mature (osteoblastic) compartments of the osteogenic lineage. Continued recruitment and accumulation of fibroblast-like, pre-osteogenic cells would then result in the fibrosis of marrow spaces adjacent to bone surfaces.

### Acknowledgments

We thank Dr. P. K. Patel, Children's Memorial Hospital (Chicago, IL), for providing us with fresh patient material for this study and the Pathology Departments of Children's Hospital (Boston, MA), Massachusetts General Hospital (Boston, MA), and Baptist Medical Center (Columbia, SC) for their help in obtaining patient specimens.

### References

1. Albright F, Butler AM, Hampton AO, Smith P: Syndrome characterized by osteitis fibrosa disseminata, areas of pigmentation and endocrine dysfunction with precocious puberty in females. *N Engl J Med* 1937, 216:727-746
2. Danon M, Crawford JD: The McCune-Albright syndrome. *Ergeb Inn Med Kinderheilkd* 1987, 55:81-115
3. Weinstein LS, Shenker A, Gejman PV, Merino MJ, Friedman E, Spiegel AM: Activating mutations of the stimulatory G protein in the McCune-Albright Syndrome. *N Engl J Med* 1991, 325:1688-1695
4. Schwindinger WF, Francomano CA, Levine MA: Identification of a mutation in the gene encoding the  $\alpha$  subunit of the stimulatory G protein of adenyl cyclase in McCune-Albright syndrome. *Proc Natl Acad Sci USA* 1992, 89:5152-5156
5. Shenker A, Weinstein LS, Moran A, Pescovitz OH, Charest NJ, Boney CM, Van Wyk JJ, Merino MJ, Feuillan PP, Spiegel AM: Severe endocrine and nonendocrine manifestations of the McCune-Albright syndrome associated with activating mutations of stimulatory G protein  $Gs$ . *J Pediatr* 1993, 123:509-518
6. Malchoff CD, Reardon G, MacGillivray DC, Yamase H, Rogol AD, Malchoff DM: An unusual presentation of McCune-Albright syndrome confirmed by an activating mutation of the  $Gs$   $\alpha$ -subunit from a bone lesion. *J Clin Endocrinol Metab* 1994, 78:803-806
7. Shenker A, Weinstein LS, Sweet DE, Spiegel AM: An activating  $Gs$   $\alpha$  mutation is present in fibrous dysplasia of bone in the McCune-Albright syndrome. *J Clin Endocrinol Metab* 1994, 79:750-755
8. Candelieri GA, Glorieux FH, Prud'homme J, St-Arnaud R: Increased expression of the c-fos proto-oncogene in bone from patients with fibrous dysplasia. *N Engl J Med* 1995, 332:1546-1551



9. Yamamoto T, Ozono K, Kasayama S, Yoh K, Hiroshima K, Takagi M, Matsumoto S, Michigami T, Yamaoka K, Kishimoto T, Okada S: Increased IL-6 production by cells isolated from the fibrous bone dysplasia tissues in patients with McCune-Albright syndrome. *J Clin Invest* 1996, 98:30-35
10. Marie PJ, de Pollak C, Chanson P, Lomri A: Increased proliferation of osteoblastic cells expressing the activating Gs  $\alpha$  mutation in monostotic and polyostotic fibrous dysplasia. *Am J Pathol* 1997, 150:1059-1069
11. Shenker A, Chanson P, Weinstein LS, Chl P, Spiegel AM, Lomri A, Marie PJ: Osteoblastic cells derived from isolated lesions of fibrous dysplasia contain activating somatic mutations of the Gs  $\alpha$  gene. *Hum Mol Genet* 1995, 4:1675-1676
12. Alman BA, Grell DA, Wolfe HJ: Activating mutations of Gs protein in monostotic fibrous lesions of bone. *J Orthop Res* 1996, 14:311-315
13. Bianco P, Boyde A: Alkaline phosphatase cytochemistry in confocal scanning light microscopy for imaging the bone marrow stroma. *Basic Appl Histochem* 1989, 33:17-23
14. Fisher LW, Stubbs JTR, Young MF: Antisera and cDNA probes to human and certain animal model bone matrix noncollagenous proteins. *Acta Orthop Scand Suppl* 1995, 266:61-65
15. Simonds WF, Goldsmith PK, Woodard CJ, Unson CG, Spiegel AM: Receptor and effector interactions of Gs: functional studies with antibodies to the  $\alpha$  s carboxyl-terminal decapeptide. *FEBS Lett* 1989, 249:189-194
16. Gehron Robey P, Bianco P, Termine JD: The cellular biology and molecular biochemistry of bone formation. *Disorders of Bone and Mineral Metabolism*. Edited by Coe FL, Favus MJ. New York, Raven Press, 1992, pp 241-263
17. Bianco P, Riminucci M, Bonucci E, Termine JD, Gehron Robey P: Bone sialoprotein (BSP) and osteoblast differentiation: relationship to alkaline phosphatase, bromodeoxyuridine incorporation, and matrix deposition. *J Histochem Cytochem* 1993, 41:183-191
18. Gehron Robey PG, Termine JD: Human bone cells in vitro. *Calcif Tissue Int* 1985, 37:453-460
19. Owen M: The origin of bone cells. *Int Rev Cytol* 1970, 28:213-238
20. Greco MA, Steiner GC: Ultrastructure of fibrous dysplasia of bone: a study of its fibrous, osseous, and cartilaginous components. *Ultrastruct Pathol* 1986, 10:55-66
21. Bianco P: Structure and mineralization of bone. *Mineralization in Biological Systems*. Edited by Bonucci E. Boca Raton, FL, CRC Press, 1992, pp 243-268
22. Miller SS, Wolf AM, Arnaud CD: Bone cells in culture: morphologic transformation by hormones. *Science* 1976, 192:1340-1343
23. Ferdario NS, Termine JD, Young MF, Robey PG: Temporal regulation of hyaluronan and proteoglycan metabolism by human bone cells in vitro. *J Biol Chem* 1990, 265:12200-12209
24. Bianco P, Fisher LW, Young MF, Termine JD, Robey PG: Expression and localization of the two small proteoglycans biglycan and decorin in developing human skeletal and non-skeletal tissues. *J Histochem Cytochem* 1990, 38:1549-1563
25. Bianco P, Silvestrini G, Termine JD, Bonucci E: Immunohistochemical localization of osteonectin in developing human and calf bone using monoclonal antibodies. *Calcif Tissue Int* 1988, 43:155-161
26. Bianco P, Fisher LW, Young MF, Termine JD, Robey PG: Expression of bone sialoprotein (BSP) in developing human tissues. *Calcif Tissue Int* 1991, 49:421-426
27. Mark MP, Butler WT, Prince CW, Finkelman HD, Ruch JV: Developmental expression of 44-kd bone phosphoprotein (osteopontin) and bone  $\gamma$ -carboxyglutamic acid (Gla)-containing protein (osteocalcin) in calcifying tissues of rat. *Differentiation* 1988, 37:123-136
28. Mintz KP, Orzesik WJ, Midura RJ, Robey PG, Termine JD, Fisher LW: Purification and fragmentation of nondenatured bone sialoprotein: evidence for a cryptic, RGD-resistant cell attachment domain. *J Bone Miner Res* 1993, 8:985-995
29. Denhardt DT, Lopez CA, Rolla FE, Hwang SM, An XR, Walther SE: Osteopontin-induced modifications of cellular functions. *Ann NY Acad Sci* 1995, 760:127-142
30. Rodan GA, Martin TJ: Role of osteoblasts in hormonal control of bone resorption: a hypothesis. *Calcif Tissue Int* 1981, 33:349-351
31. Bianco P, Bonucci E: Endosteal surfaces in hyperparathyroidism: an enzyme cytochemical study on low temperature processed glycol methacrylate embedded bone biopsies. *Virchows Arch A Pathol Anat Histopathol* 1991, 419:425-431
32. Kopp JB, Robey PG, Termine JD: Osteonectin promoter: DNA sequence analysis and S1 endonuclease site potentially associated with transcriptional control in bone cells. *J Biol Chem* 1989, 264:450-456
33. Ken JM, Fisher LW, Termine JD, Wang MG, McBride OW, Young MF: The human bone sialoprotein gene (IBSP): genomic localization and characterization. *Genomics* 1993, 17:408-415
34. Everitt EA, Sage EH: Expression of SPARC is correlated with altered morphologies in transfected F9 embryonal carcinoma cells. *Exp Cell Res* 1992, 199:134-146
35. Noda M, Rodan GA: Transcriptional regulation of osteopontin production in rat osteoblast-like cells by parathyroid hormone. *J Cell Biol* 1989, 108:713-718